Crystallization Kinetics of Polypropylene Composites Filled with Nano Calcium Carbonate Modified with Maleic Anhydride

Hai Huang,[1] Bing Han,[2] Lei Wang,[1] Ning Miao,[1] Hong Mo,[1] Ning-Lin Zhou,[1] Zhen-Mao Ma,[1] Jun Zhang,[1] Jian Shen[1,3]

[1]*Jiangsu Engineering Research Center for Biomedical Function Materials, College of Chemistry and Environment Science, Nanjing Normal University, Nanjing 210097, People's Republic of China*
[2]*College of Materials Science and Engineering, Nanjing Institute of Technology, Nanjing 211167, People's Republic of China*
[3]*Research Center of Surface and Interface Chemistry and Chemical Engineering Technology, Nanjing University, Nanjing 210093, People's Republic of China*

Received 22 January 2010; accepted 10 May 2010
DOI 10.1002/app.32842
Published online 19 August 2010 in Wiley Online Library (wileyonlinelibrary.com).

ABSTRACT: The subject of this study was the crystallization behavior and thermal properties of polypropylene (PP)/maleic anhydride (MAH) modified nano calcium carbonate (nano-$CaCO_3$) composites. In this study, 5 wt % nano-$CaCO_3$ modified with different contents of MAH was filled into a PP matrix. X-ray diffraction and differential scanning calorimetry were used to characterize the crystal morphology and crystallization kinetics of a series of composites. The results demonstrate that the nano-$CaCO_3$ modified with MAH had an important effect on the thermal and morphological properties of the nanocomposites. The Avrami exponent of the pure PP was an integer, but those of the composites were not integers, but the crystallization rate constant decreased as the content of MAH in the nano-$CaCO_3$ filler increased in isothermal crystallization. In nonisothermal crystallization, the kinetic parameter $F(T)$ and the degree of crystallinity of pure PP were compared with those of the PP composites filled with nano-$CaCO_3$. We suggest that heterogeneous nucleation existed in the PP composites and that the transformation and retention of the β-form crystal into the α-form crystal took place in the composite system and the β-form crystal had a higher nucleation rate and growth process than the α-form crystal in the PP composites. © 2010 Wiley Periodicals, Inc. J Appl Polym Sci 119: 1516–1527, 2011

Key words: kinetics (polym.); plastics; poly(propylene) (PP); surface modification kinetics

INTRODUCTION

Polypropylene (PP) is a typical commodity polymer with many application areas and a remarkable growth rate. Because of not only its favorable price and low weight but also its extraordinary versatility in terms of properties and recycling use, PP blends and composites are used in large quantities in many applications, such as the automotive electronics industry, furniture production, and many other fields. However, there exist some disadvantages, including a high molding shrinkage factor, poor mechanical properties, and low fracture toughness, which limit the widening of the applications of PP.[1–4] Because of these disadvantages, PP would benefit from filling modification.

In the combination of PP with other polymers, fillers or reinforcements could help improve the mechanical and structural properties and extend its applications.[5–8] Although a great number of materials have been used or at least tested as fillers or reinforcements for PP, only three have real practical importance: talc, glass fiber, and $CaCO_3$. $CaCO_3$ is the filler most commonly added to PP to improve its mechanical properties and heat stability.[9] However, good adhesion does not exist between the fillers and thermoplastic matrices. As a nonpolar substance, PP cannot easily combine with the polar $CaCO_3$. Furthermore, when the particle size of $CaCO_3$ measures up to the nanometer, the defect is much more obvious: with decreasing particle size, the surface atomicity increases, and both the surface free energy and the adsorption become stronger, so it is difficult to get good dispersion in the PP matrix because of particle reunification. Therefore, to improve the properties of the nanocomposite, it is necessary to

Correspondence to: J. Zhang (zhangjun3@njnu.edu.cn) or J. Shen (peak8844@yeah.net).
Contract grant sponsor: China National Science Foundation; contract grant number: 20874047.
Contract grant sponsor: Natural Science Foundation of the Jiangsu Higher Education Institutions of China; contract grant number: 08KJB150010.

investigate the surface modification of nano calcium carbonate (nano-$CaCO_3$).

The crystallization behavior of crystalline polymers is greatly influenced by the molecular structure and crystallization conditions. Various factors affect the mechanical properties and dominant fracture toughness micromechanisms of PP, among these crystalline morphology/structure and additives, which incorporate into the matrix, play a more important role in the system. In addition, many related reports have indicated that the crystallization property of polymer composites is determined by the size and surface properties of the fillers to a large extent.[10–27]

In a former study, we investigated the modification of nano-$CaCO_3$ with maleic anhydride (MAH).[28] In this study, we examined the crystallization behavior of the composites. Moreover, the kinetics of the nucleation and crystal growth of PP composites filled with nano-$CaCO_3$ modified with MAH were the focus of this study.

EXPERIMENTAL

Materials

$Ca(OH)_2$ and MAH were obtained from Shanghai Chemistry Reagent Co., Ltd. (Shanghai, China). CO_2 was food grade.

The modified nano-$CaCO_3$ was obtained in our previous study.[28]

The unfilled PP used as matrices were provided by Yangtze Chemical Industry Co., Ltd. (Nanjing, China).

Sample preparation

In our previous study, we obtained nano-$CaCO_3$ modified with MAH,[28] the samples of which are listed in Table I.

The nano-$CaCO_3$, which was modified with relatively different contents of MAH, was filled into PP at 5 wt %. The PP/nano-$CaCO_3$ samples were blended in a Haake torque rheometer (Polylab 600) provided by Thermo Fisher Scientific, Inc., Waltham MA, USA). The mixing conditions were as follows: the speed was 60 rpm, the temperature was 230°C, and the time was 10 min. The sample volume of each blending was 49 cm^3.

The ultimate PP composite relationship between the composite number and filler number can be seen in Table I.

TABLE I
Relationship Between the PP/Nano-$CaCO_3$ Composite Number and the Content of MAH in the Nano-$CaCO_3$ Filler

Filler number	1′	2′	3′	4′	5′
Content of MAH (%)	1.0	1.5	2.0	2.5	3.0
Composite number	1	2	3	4	5

X-ray diffraction (XRD) measurements

XRD analysis was carried out with a Rigaku D/max-rc X-ray diffractometer (Rigaku Co., Tokyo, Japan). The testing voltage was 30 kV, and the current was 20 mA.

Cu Kα wire ($\lambda = 0.15418$ nm) and a nickel filter clogging plate were also used with the scanning range of 0.5–40° (2θ). The samples were injected and tested at room temperature.

Differential scanning calorimetry (DSC) measurements

The melting and crystalline behaviors of pure PP and samples 1–5 were measured with a PerkinElmer DSC-7 (PerkinElmer, Inc., Wellesley, MA, USA). First, pure PP and samples 1–5 were heated from room temperature to 190°C and held at 190°C for 10 min to eliminate all of the thermal history in the materials. Then, the samples were cooled to 50°C at a cooling rate (R) of 10°C/min to obtain their crystalline characteristics. Last, the samples were heated to 190°C at a heating rate of 10°C/min to obtain their melting characteristics. All of the operations were performed under a nitrogen flow. The sample weight was in the range 4–5 mg.

During the isothermal crystallization kinetic measurements, the samples were heated from room temperature to 190°C at a heating rate of 50°C/min, and held at 190°C for 10 min to eliminate all of the thermal history in the materials. Then, the samples were cooled rapidly at $R = 200$°C/min to crystallization temperatures (T_c's) of 122, 124, 126, 128, and 130°C/min and held at these temperatures for the entire crystallization process.

During the nonisothermal crystallization kinetic measurements, the samples were heated from room temperature to 190°C at a heating rate of 50°C/min and held at 190°C for 10 min to eliminate all of the thermal history in the materials. Then, the samples were cooled to crystallize at the selected constant rates (from 5 to 40°C/min). All of the operations were performed under a nitrogen purge.

Attenuated total reflection (ATR)–IR spectroscopy

The MAH and the active $CaCO_3$ samples were fully dried to a constant weight, and then, their surfaces were characterized by a Nexus 870 IR spectrometer (Thermo Fisher Nicokt Co., USA) with ATR, and the testing range was 650–4000 cm^{-1}.

RESULTS AND DISCUSSION

XRD characterization

The crystallization behavior of composites is strongly influenced by the dispersion state of the

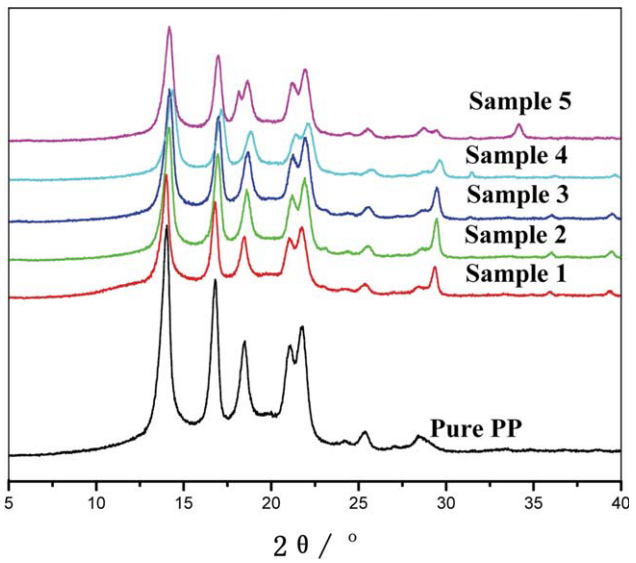

Figure 1 XRD patterns of pure PP and samples 1–5. [Color figure can be viewed in the online issue, which is available at wileyonlinelibrary.com.]

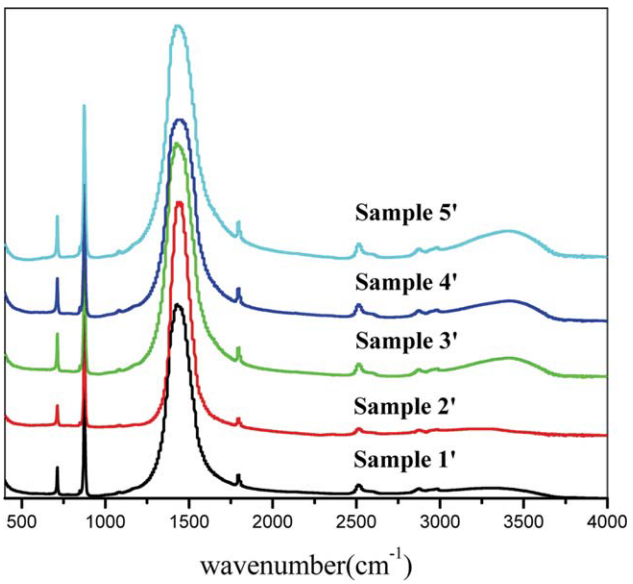

Figure 2 ATR–FTIR spectrum of different nano-$CaCO_3$ samples modified with MAH. [Color figure can be viewed in the online issue, which is available at wileyonlinelibrary.com.]

nanoparticles in the polymer matrix, which can be analyzed by XRD.[29] It is well known that PP can crystallize into different crystalline polymorphs, that is, the monoclinic α form, the trigonal β form, and the triclinic γ form. The main Bragg reflections at 2θ angles of 14.0, 16.8, and 18.4° correspond to the (110), (040), and (130) planes of the α form, respectively.[30] Figure 1 shows the XRD patterns of pure PP and samples 1–5. As shown in Figure 1, pure PP crystallized in the monoclinic α form, and samples 1–2 were similar, but the crystalline basal position peak at a 2θ angle of 18.4° of samples 3 and 4 became evidently broader; moreover, a shoulder peak appeared. The overall XRD results suggest that a bit of the trigonal β form was generated in these samples. In sample 5, a double peak at the characteristic crystalline basal position peak of the β form suggested that the nano-$CaCO_3$ modified with MAH could induce the composites to crystallize in β form, and the content of the β form increased with increasing MAH content in the composites. This was explained by the hydroxide radical on the surface of the modified nano-$CaCO_3$, which had an effect on the transformation and retention of the β-form crystal into the α-form crystal in the composite system.

Indirect observation by ATR–Fourier transform infrared (FTIR) spectroscopy was then necessary to characterize an exfoliation state. Figure 2 presents the ATR–FTIR spectrum of different nano-$CaCO_3$ modified with MAH.The peaks at 1790 cm^{-1} were attributed to C=O, but as we all know, there are no peaks in pure $CaCO_3$; this indicated that the modified nano-$CaCO_3$ was definitely associated with the features of the functional groups. In addition, characteristic absorption peaks appeared at 3450 cm^{-1} in samples 3′–5′ but not in samples 1′ and 2′, and the intensity of the absorption peak increased with the content of MAH (from 3′ to 5′). This could have indicated that this was the hydroxide radical on the samples, which were fully dried to eliminate the influence of water. So, this could have indicated that the hydroxide radical affected the transformation and retention of the β-form crystal into the α-form crystal.

The crystallinity (X_c) of PP is defined by the following equation:

$$X_c = \frac{I_c}{I_a + I_c}$$

where I_c is the crystalline area of XRD and I_a is the amorphous area of XRD.

Table II lists the crystallinity of pure PP and samples 1–5. It shows that the samples 1–5 had a higher

TABLE II
Crystallinity Values of Pure PP and Samples 1–5

	Sample					
	Pure PP	Sample 1	Sample 2	Sample 3	Sample 4	Sample 5
Crystallinity (%)	60.9	64.5	66.5	67.5	63.0	69.8

TABLE III
DSC Data of the PP Composites Filled with Nano-$CaCO_3$ Modified with Different Contents of MAH and Pure PP (10°C/min)

Sample	T_c (°C)	T_m (°C)	ΔT (°C)
Pure PP	113. 6	156.9	43.3
1	113.9	159.6	45.7
2	112.7	156.7	44.0
3	117.7	157.4	39.7
4	117.3	157.0	39.7
5	118.2	158.4	40.2

crystallinity than pure PP, and sample 5 was the largest. This implied that the induced crystallization had an effect on the crystallinity and that the transformation and retention of the β-form crystal into α-form crystal in the composite system took place.

Crystallization process and crystal morphology

The effect of the fillers on the melting and crystallization properties of PP was analyzed in nonisothermal DSC experiments at a rate of 10°C/min. Table III

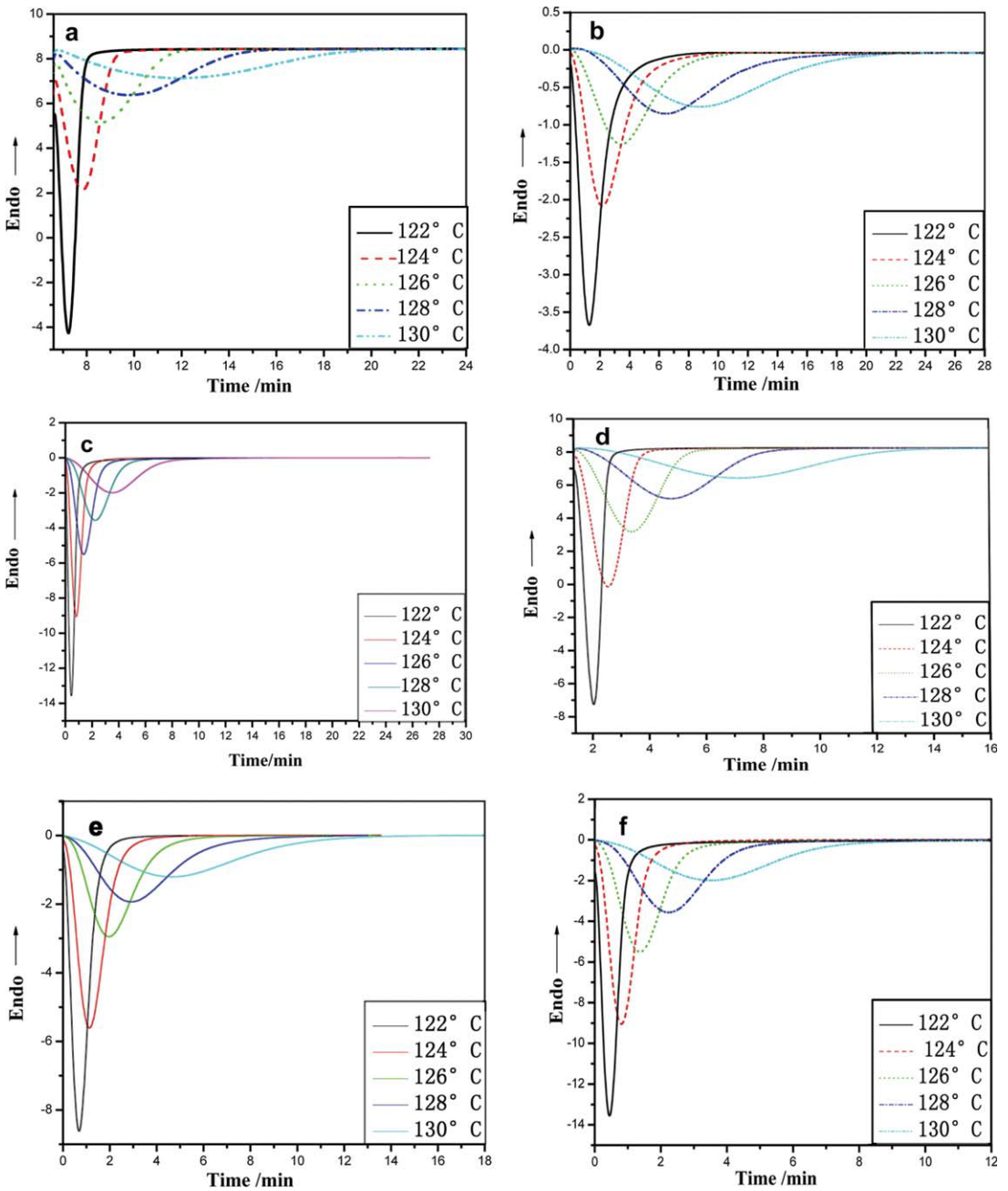

Figure 3 Isothermal crystallization curves of five kinds of composites and pure PP: (a) pure PP and samples (b) 1, (c) 2, (d) 3, (e) 4, and (f) 5. [Color figure can be viewed in the online issue, which is available at wileyonlinelibrary.com.]

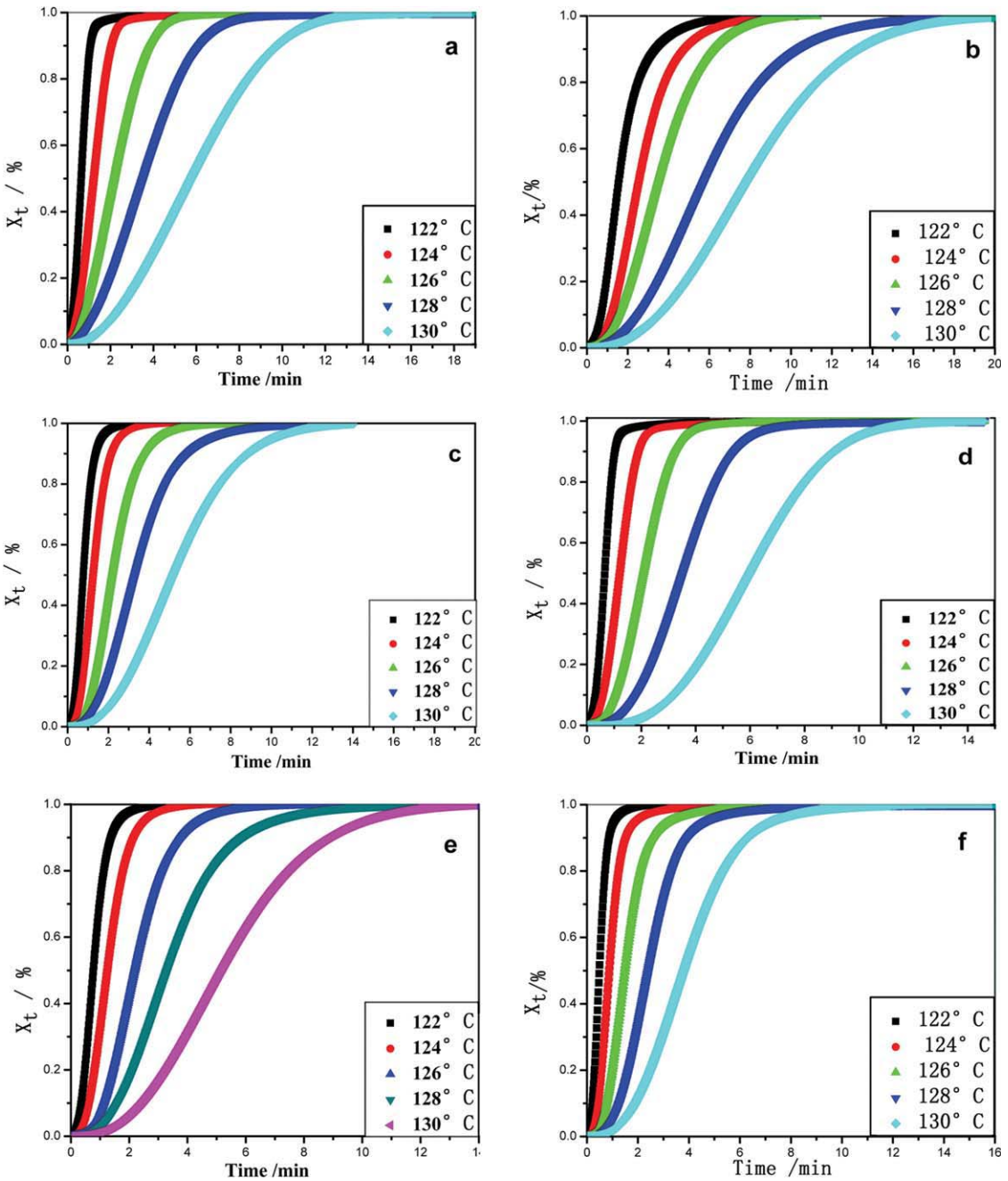

Figure 4 Plot of X_t versus the crystallization time of pure PP and five kinds of composite materials: (a) pure PP and samples (b) 1, (c) 2, (d) 3, (e) 4, and (f) 5. [Color figure can be viewed in the online issue, which is available at wileyonlinelibrary.com.]

lists the DSC results of pure PP and samples 1–5. Table III shows that the T_c of pure PP and samples 1 and 2 was obviously lower than that of samples 3–5, but the melting temperature (T_m) and ΔT ($\Delta T = T_m - T_c$) did not present obviously low. From the results of XRD, we could see that the β-form crystal formed and was retained in samples 3–5 but not in pure PP or samples 1 or 2. So, the difference in T_c among pure PP, samples 1 and 2, and samples 3–5 was attributed to the fact that the β-form crystal had a higher T_c than the α-form crystal.

Isothermal crystallization kinetics

Most studies of polymer crystallization rely on the Avrami equation[31–33] to analyze the data, which provides the information of nucleation and the crystallization rate:

$$1 - X(t) = \exp(-Kt^n) \quad (1)$$

where $X(t)$ is the volume fraction of crystalline materials at a time t, and at a given temperature T, n is the Avrami exponent and K is the crystallization

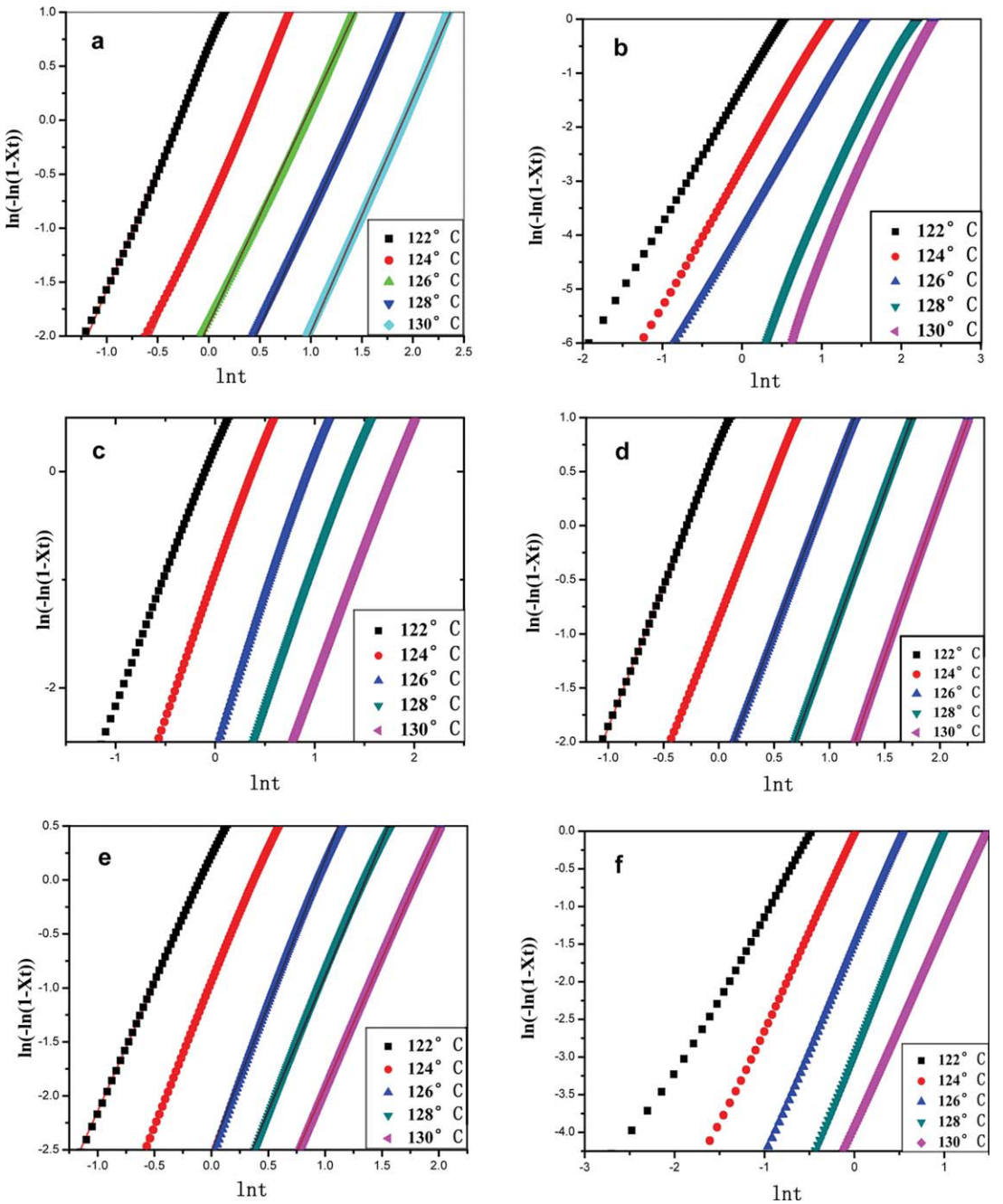

Figure 5 Plot of ln[−ln(1 − X_t)] versus ln t of five kinds of composites and pure PP: (a) pure PP and samples (b) 1, (c) 2, (d) 3, (e) 4, and (f) 5. [Color figure can be viewed in the online issue, which is available at wileyonlinelibrary.com.]

rate constant. The parameters n and ln K could be obtained from the slope and the intercept of the plots of ln[−(1 − X_t)] versus ln t at different temperatures for crystallization.

Isothermal crystallization is the process in which PP is heated rapidly above its T_m, in this study at 190°C, to various temperatures, that is, 122, 124, 126, 128, and 130°C (Fig. 3), respectively, all of which were below the melting point but above the glass-transition temperature. Those temperatures were considered as the T_c's. As shown in Figure 3, an increase in the time to reach the maximum degree of crystallization was observed, and the value of the exothermic peaks became large with the increasing T_c. All of these data indicated that a longer time was required to complete the crystallization in the composites in the isothermal crystallization.

The relative degree of crystallinity at time t (X_t) was obtained from the area of the exothermic peak of isothermal crystallization analysis in DSC. The function between X_t and time t is plotted in Figure 4. The same S shape was observed in all of the curves.[34]

TABLE IV
Avrami Kinetic Parameters from the Avrami Equation for the Isothermal Crystallization of the Samples

		Sample					
		PP	1	2	3	4	5
122°C	n	2.24	2.15	2.67	2.63	2.37	2.27
	K ($\min^{-n}$)	1.93	0.251	0.171	2.14	1.25	3.50
124°C	n	2.17	2.39	2.37	2.63	2.60	2.58
	K ($\min^{-n}$)	0.466	0.0716	0.114	0.425	0.380	0.955
126°C	n	2.01	2.30	2.54	2.74	2.70	2.73
	K ($\min^{-n}$)	0.151	0.0387	0.0285	0.0942	0.0815	0.227
128°C	n	2.07	2.27	2.58	2.82	2.50	2.86
	K ($\min^{-n}$)	0.0525	0.0129	0.00716	0.0196	0.0337	0.0551
130°C	n	2.16	2.35	2.48	2.91	2.40	2.63
	K ($\min^{-n}$)	0.0162	0.00547	0.00306	0.00381	0.0133	0.0205

To deal conveniently with the operation, eq. (1) is usually rewritten in a double-logarithmic form as follows:

$$\ln[-\ln(1 - X_t)] = \ln K + n \ln t \tag{2}$$

When $\ln[-\ln(1 - X_t)]$ versus $\ln t$ was plotted for each R, as shown in Figure 5, each curve showed an almost linear relationship. This indicated that the isothermal crystallization behavior of the samples could be properly described by the Avrami equation. n and K, which are listed in Table IV, were determined from the slope and intercept of the lines. The qualitative information on the nature of nucleation and the growth processes in the composite were obtained. The n values of the composites were rough, but the K values decreased with increasing T_c. Sample 5 had the fastest nucleation rate and growth process; this was determined from the K values, which suggested that the β-form crystal had a higher nucleation rate and growth process than the α-form crystal.

As shown in Table IV, n of pure PP was about 2, whereas those of samples 1–5 were in the range 2.2–3.0. Also, the n value of sample 3 was larger than that of any other sample; in our former study, we found that sample 3′ had the biggest contact angle (Table V),[28] which indicated that the smallest surface polarity had an obvious effect on modification. Furthermore, the relation between the crystallization rate and the activation energy could be expressed by eq. (3):

$$G(T) = G_0 \exp\left(\frac{-\Delta F_D^*}{RT}\right) \exp\left(\frac{-\Delta F*}{RT}\right) \tag{3}$$

where $G(T)$ is the crystal growth rate on the crystallization temperature T; G_0 is a pre-exponential factor generally assumed to be constant or proportional to T. ΔF_D^* is the activation energy of diffusion of the polymer segment from the random coil to the crystal surface and ΔF^* is the activation energy of nucleation. The overall crystallization rate is reversely proportional to the ratio of ΔF_D^* to the difference between T_c and the glass-transition temperature and also reversely proportional to the ratio of ΔF^* to the difference between T_m and T_c. As we all know, PP is a nonpolar polymer. The higher n value of sample 3 indicated a lower ΔF, which led to nucleation more easily. Thus, the polarity reached to optimum matching between sample 3 and PP, and the PP polymer segment ranged into the crystal lattice on the surface of sample 3.

TABLE V
Contact Angle Results of Samples 1′–5′

Sample	1′	2′	3′	4′	5′
Contact angle (°)	137.5	147.5	153.0	140.2	139.0

We concluded that the isothermal crystallization of pure PP was a nucleation mode of homogeneous nucleation and a one-dimensional growth pattern, whereas the MAH–nano-$CaCO_3$ had an effect of heterogeneous nucleation in the PP composites, and parts of them grew in a type of two-dimensional nucleation.

Nonisothermal crystallization kinetics

Theoretical background

As we know, the Avrami equation can also be used to describe nonisothermal crystallization kinetics. Ozawa[35] extended the Avrami equation and put forward a new equation:

$$1 - X(t) = \exp[-K(T)/R^m]$$

where $X(t)$ is the relative crystallinity, $K(T)$ is the crystallization rate constant, and m is the Ozawa exponent. The equation is usually rewritten in a double-logarithmic form as follows:

$$\ln\{-\ln[1 - X(t)]\} = \ln K(T) + m \ln R$$

$K(T)$ is a function related to the overall crystallization rate. Mo et al.[36] combined the Avrami equation with the Ozawa equation, and the combined equation can be written as follows:

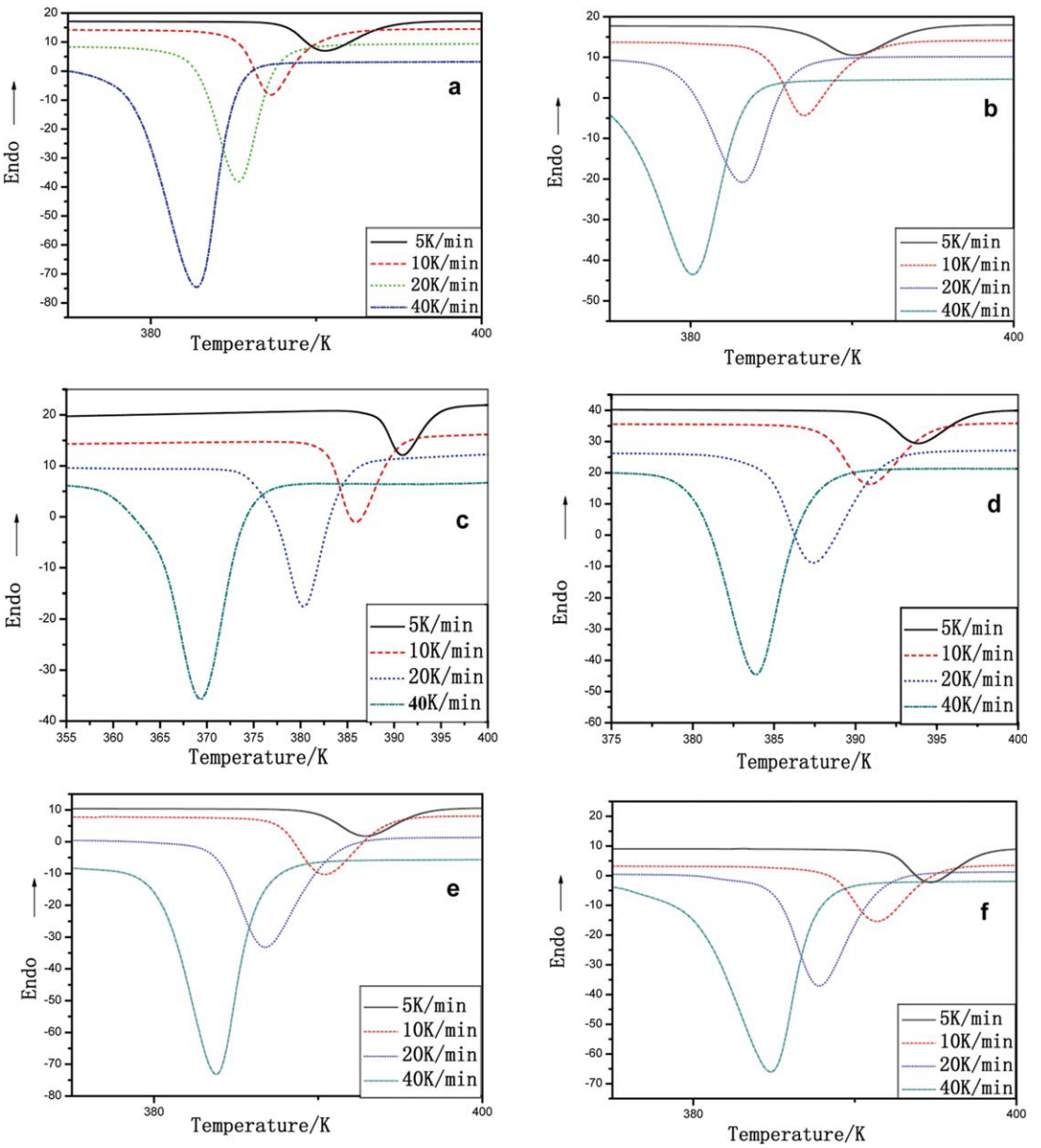

Figure 6 DSC thermo gram of pure PP and five kinds of PP composites filled with nano-$CaCO_3$ at various R values: (a) pure PP and samples (b) 1, (c) 2, (d) 3, (e) 4, and (f) 5. [Color figure can be viewed in the online issue, which is available at wileyonlinelibrary.com.]

$$\ln R = \ln F(T) - A \ln t$$

A is the rate of the Arrami exponent n to the Ozawa exponent m, and

$$F(T) = [K(T)/Z_t]^{1/m}$$

where the Mo exponent A is the ratio of n to m, that is, $A = n/m$. Jeziorny[37] corrected it by R as follows:

$$\ln Z_c = \ln Z_t / R$$

Z_t is the crystallization rate constant. Where Z_c is the kinetic crystallization rate constant. Plotting ln R versus ln t yields a linear relationship between ln R and ln t. From the intercept and slope, one can estimate the data of the kinetic parameters $F(T)$ and A. In this study, we used the Mo equation, and the results showed us that the Mo equation was effective.

Nonisothermal crystallization behavior

The nonisothermal crystallization behavior of pure PP and samples 1–5 were investigated by DSC. A PerkinElmer Pyris 7 calorimeter was used. First, a heating run from room temperature to 190°C was performed at different heating rates ranging from 5 to 40°C/min. Once the sample thermal history was erased for 5 min at 190°C, cooling cycles were conducted from 190 to 50°C, with different R values

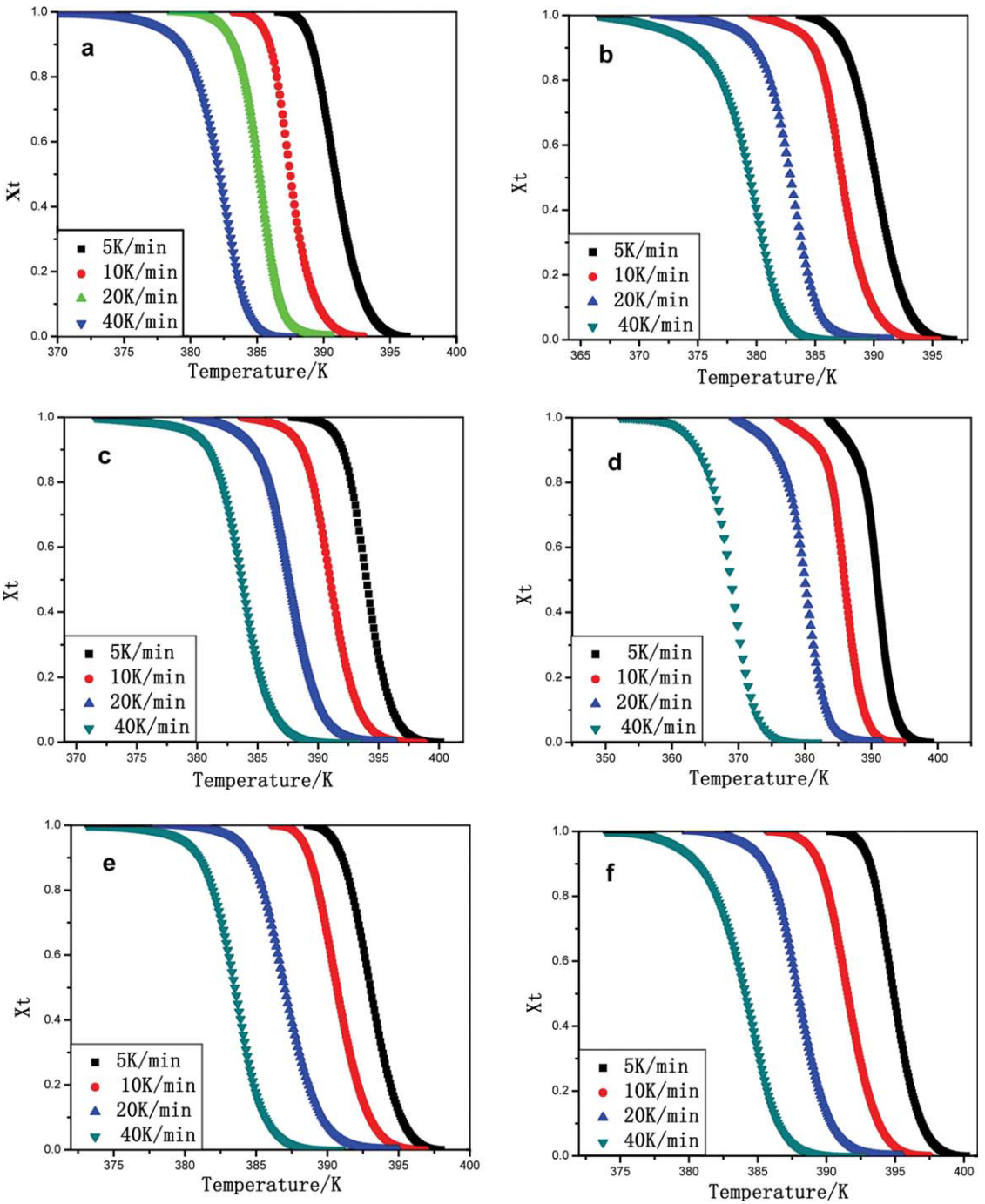

Figure 7 Plot of X_t versus T_c of pure PP and five kinds of composite materials: (a) pure PP and samples (b) 1, (c) 2, (d) 3, (e) 4, and (f) 5. [Color figure can be viewed in the online issue, which is available at wileyonlinelibrary.com.]

ranging from 5 to 40°C/min. All runs were carried out in a stream of dried nitrogen. The sample mass was typically 3 mg.

The relative degree of crystallinity as a function of temperature (X_T) can be formulated as

$$X_T = \int_{T_0}^{T} (dH/dT)dT / \int_{T_0}^{T_\infty} (dH/dT)/dT \qquad (4)$$

where dH denotes the measured enthalpy of crystallization during an infinitesimal temperature interval (dT). The limits T_0 and T_∞ are used to denote the elapsed ΔT during the course of crystallization and at the end of the crystallization process, respectively.

Again, T_c can be converted to crystallization time as shown:

$$t = (T_0 - T_c)/R \qquad (5)$$

In our study, Figure 6 shows the DSC thermogram of pure PP and five kinds of PP composites at various R values; we found that in the melt

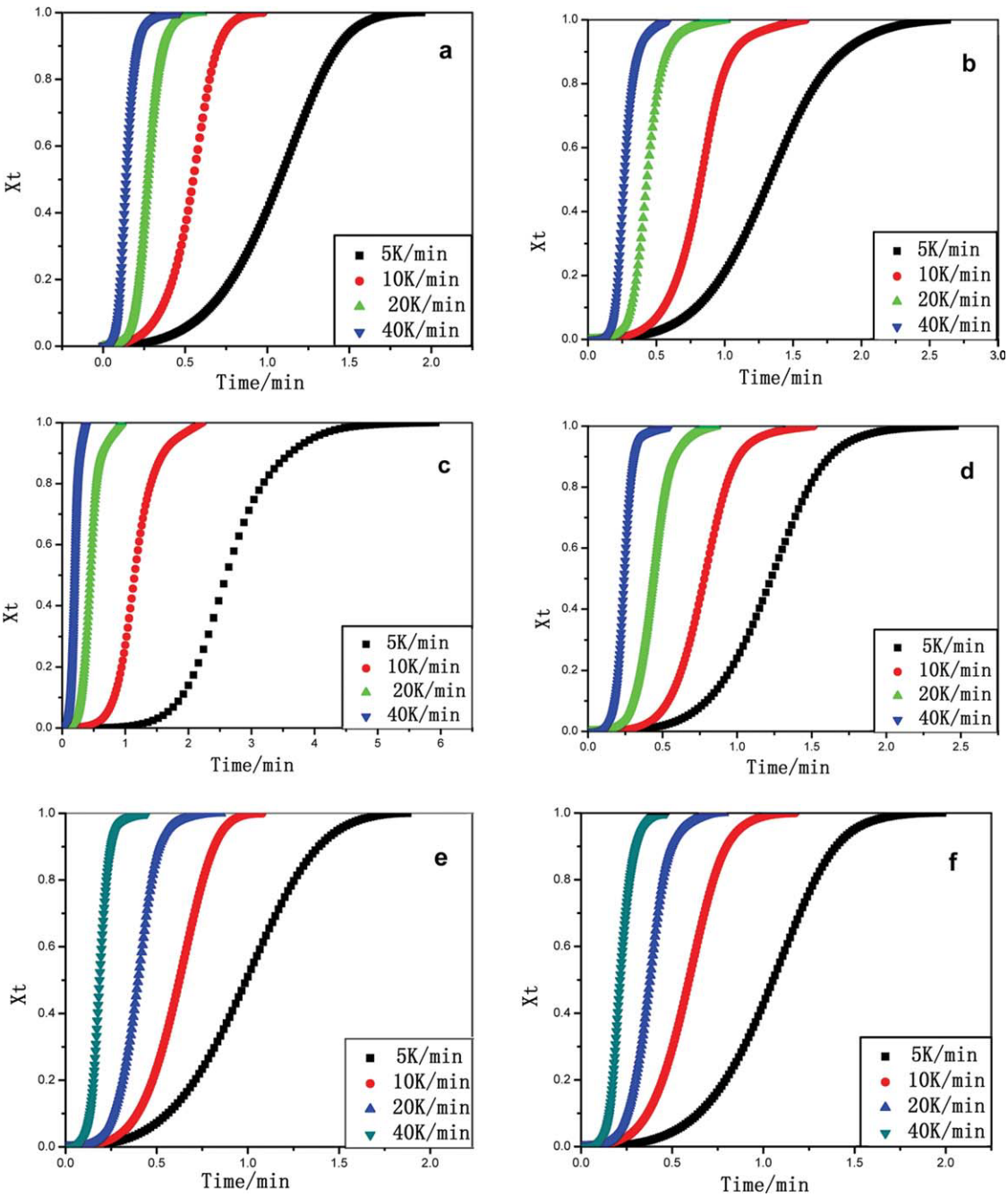

Figure 8 Plot of X_t versus the crystallization time of pure PP and five kinds of composite materials: (a) pure PP and samples (b) 1, (c) 2, (d) 3, (e) 4, and (f) 5. [Color figure can be viewed in the online issue, which is available at wileyonlinelibrary.com.]

crystallization, the crystallization peak shifted to lower temperatures as the R value increased.

From Figure 6, with eq. (3), we obtained Figure 7, which shows X_t versus T_c. Likewise, the relation between X_t and the crystallization time is shown in Figure 8.

If the Ozawa method is valid, we should have obtained a plot of $\log\{-\ln[1 - X(t)]\}$ versus $\log R$ resulting in a straight line.[38] However, the straight line was not obtained in our experiment. Then, we used the Mo equation,[36] the plots of $\ln R$ versus $\ln t$ for the nonisothermal crystallization of the pure PP and five kinds of composite materials at various relative crystallinities, as shown in Figure 9. Obviously, the linearity was good, which indicated that the Mo method was effective.

$F(T)$ has a definite physical and practical meaning: the smaller the value of $F(T)$ is, the higher the crystallization rate becomes. The values of $F(T)$ and A could be obtained from the intercept and slope of the straight

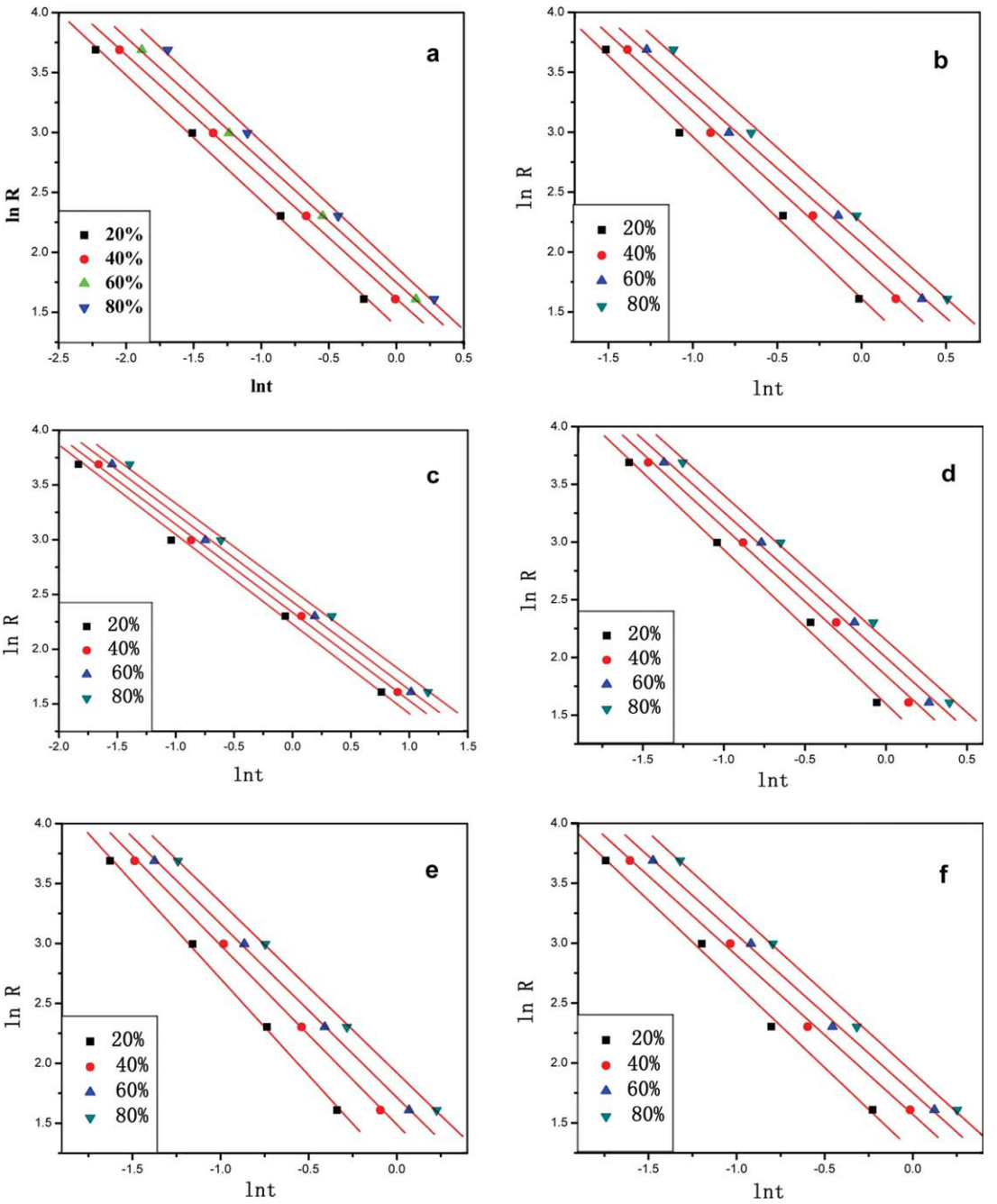

Figure 9 Plots of ln R versus ln t of pure PP and five kinds of composite materials: (a) pure PP and samples (b) 1, (c) 2, (d) 3, (e) 4, and (f) 5. [Color figure can be viewed in the online issue, which is available at wileyonlinelibrary.com.]

lines, respectively, and are tabulated in Table VI. The values of $F(T)$ of the five samples increased with increasing relative degree of crystallinity. Also, the values of A increased slightly; this indicated that the ratio of crystallization between 5 and 40°C/min remained constant whatever the relative crystallinity. However, the values of $F(T)$ of pure PP decreased when the relative degree of crystallinity was 60%; this suggested that secondary crystallization may have played a partial role in the PP composites. Moreover, in Figure 9, according to the equation $A = n/m$, we indicate that the value of m was the highest in the sample because the n value of sample 3 was the highest in the isothermal crystallization. These results were in agreement with the isothermal crystallization behavior discussed previously.

CONCLUSIONS

1. The hydroxide on the surface of nano-$CaCO_3$ affected the formation and retention of the β-form crystal of PP.

TABLE VI
Values of *A* and *F*(*T*) from the Mo Equation at Different Temperatures of Nonisothermal Crystallization for Pure PP and the PP Composites

X(*t*) (%)	*F*(*T*)	*A*
Pure PP		
20	0.351	1.38
40	0.362	1.61
60	0.360	1.75
80	0.350	1.88
Sample 1		
20	0.259	1.61
40	0.276	1.89
60	0.287	2.08
80	0.284	2.24
Sample 2		
20	0.441	2.23
40	0.447	2.34
60	0.448	2.43
80	0.453	2.54
Sample 3		
20	0.263	1.60
40	0.278	1.84
60	0.284	2.00
80	0.285	2.15
Sample 4		
20	0.199	1.09
40	0.224	1.49
60	0.235	1.72
80	0.241	1.92
Sample 5		
20	0.248	1.26
40	0.265	1.57
60	0.268	1.76
80	0.264	1.92

2. The T_c values of samples 3–5 were obviously higher than that of pure PP and samples 1 and 2, because of which the β-form crystal had a higher T_c than the α-form crystal.
3. The results of isothermal crystallization kinetics show that pure PP exhibited a one-dimensional growth pattern and homogeneous nucleation, but the PP composites showed contrary results, which were related to the heterogeneous nucleation effect of MAH–nano-$CaCO_3$, and the β-form crystal had a higher nucleation rate and growth process than the α-form crystal in the PP composites. This resulted in the crystallinity of samples 1–5 being higher than that of pure PP.
4. The nonisothermal crystallization kinetics were the same as the isothermal crystallization kinetics. The Mo method successfully dealt with the nonisothermal process crystallization behavior.

References

1. Collar, E. P.; Laguna, O.; Areso, S.; García-Martínez, J. M. Eur Polym J 2003, 39, 157.
2. Moore, E. P. Polypropylene Handbook; Hanser: Munich, 1996.
3. Li, Q. L.; Jiang, P. J.; Su, Z. P.; Wei, P.; Wang, G. L.; Tang, X. Z. J Appl Polym Sci 2005, 96, 854.
4. Chung, M. J.; Jang, L. W.; Shim, J. H.; Yoon, J. S. J Appl Polym Sci 2005, 95, 307.
5. Torres, F. G.; Bush, S. F. Compos A 2000, 31, 1289.
6. Xu, T.; Lei, H.; Xie, C. S. Polym Test 2002, 21, 319.
7. Gamstedt, E. K.; Berglund, L. A.; Ton, P. Compos Sci Technol 1999, 59, 759.
8. Premalal, H. G. B.; Ismail, H.; Baharin, A. Polym Test 2002, 21, 833.
9. Öksüz, M.; $Y_1ld_{1r1}m$, H. J Appl Polym Sci 2005, 96, 1127.
10. Sole, B. M.; Ball, A. Tribol Int 1996, 29, 457.
11. Riley, A. M.; Paynter, C. D.; McGenity, P. M.; Adams, J. M. Plast Rubber Process Appl 1990, 14, 85.
12. Jilken, L.; Malhammar, G.; Selden, R. Polym Test 1991, 10, 329.
13. Mareri, P.; Bastide, S.; Binda, N.; Crespy, A. Compos Sci Technol 1998, 58, 747.
14. Cho, J. W.; Paul, D. R. Polymer 2001, 42, 1083.
15. Khunova, V.; Hurst, J.; Janigova, I.; Smatko, V. Polym Test 1999, 18, 501.
16. Tjong, S. C. Mater Sci Eng R 2006, 53, 73.
17. Strawhecker, K. E.; Manias, E. Chem Mater 2000, 12, 2943.
18. Zebarjad, S. M.; Tahani, M.; Sajjadi, S. A. J. Mater Proc Tech 2004, 155/156, 1459.
19. Karger-Kocsis, J. In Polypropylene, Structure, Blends and Composites; Karger-Kocsis, J., Ed.; Chapman & Hall: London, 1995; Vol. 3, p 142.
20. Pukanszky, B.; Belina, K.; Rockaebauer, A.; Maurer, F. H. J. Composites 1994, 25, 205.
21. McGenity, P. M.; Hooper, J. J.; Paynter, C. D.; Riley, A. M.; Nutbeem, C.; Elton, N. J.; Adams, J. M. Polymer 1992, 33, 5215.
22. Lin, Z. D.; Huang, Z. Z.; Zhang, Y.; Mai, K. C.; Zeng, H. M. J Appl Polym Sci 2004, 91, 2443.
23. Zhu, W. P.; Zhang, G. P.; Yu, J. Y.; Dai, G. J Appl Polym Sci 2004, 91, 431.
24. Ansari, D. M.; Price, G. J. J Appl Polym Sci 2003, 88, 1951.
25. Zhang, Q. X.; Yu, Z. Z.; Xie, X. L.; Mai, Y. W. Polymer 2004, 45, 5985.
26. Zhang, J.; Ding, Q. J.; Zhou, N. L.; Li, L.; Ma, Z. M.; Shen, J. J Appl Polym Sci 2006, 101, 2443.
27. Labour, T.; Vigier, G.; Séguéla, R.; Gauthier, C.; Orange, G.; Bomal, Y. J Polym Sci Part B: Polym Phys 2002, 40, 31.
28. Zhang, J.; Bao, F. R.; Dai, D. P.; Zhou, N. L.; Li, L.; Lu, S.; Shen, J. Chin J Inorg Chem 2007, 5, 825.
29. Vermogen, A.; Masenelli-Varlot, K.; Seguela, R.; Duchet-Rumeau, J.; Boucard, S.; Prele, P. Macromolecules 2005, 38, 9661.
30. Naffakh, M.; Martín, Z.; Marco, C.; Gómez, M. A.; Jiménez, I. Thermochim Acta 2008, 472, 15.
31. Avrami, M. J Chem Phys 1939, 7, 1103.
32. Avrami, M. J Chem Phys 1940, 8, 212.
33. Avrami, M. J Chem Phys 1941, 9, 177.
34. Zou, P.; Tang, S. W.; Fu, Z. Z.; Xiong, H. G. Int J Therm Sci 2009, 48, 837.
35. Ozawa, T. Polymer 1971, 12, 150.
36. Liu, T. X.; Mo, Z. S.; Wang, Z. S.; Zhang, H. F. Polym Eng Sci 1997, 37, 568.
37. Jeziorny, A. Polymer 1978, 19, 1142.
38. Liu, H. Z.; Yang, G. S.; He, A. H.; Wu, M. Y. J Appl Polym Sci 2005, 94, 824.